



CrossMark
 click for updates

Cite this: *RSC Adv.*, 2015, 5, 64886

Azo-containing asymmetric bent-core liquid crystals with modulated smectic phases†

Nemanja Trišović,^{*a} Jelena Antanasijević,^a Tibor Tóth-Katona,^b Michal Kohout,^c Mirosław Salamonczyk,^{d,e} Samuel Sprunt,^e Antal Jáklí^d and Katalin Fodor-Csorba^b

A new series of azo-containing bent-core liquid crystals derived from 3-hydroxybenzoic acid has been synthesized. Their mesomorphic properties have been characterized by polarizing optical microscopy, differential scanning calorimetry, small-angle X-ray diffraction and electro-optic studies. Almost all the compounds form an enantiotropic modulated smectic (B₇ type) phase over relatively broad temperature ranges. Structural modifications, such as the type and length of the terminal chains, the rigidity of wings, and the presence of a Cl-substituent in different positions of the bent core, affect the appearance and temperature range, but not the type of the mesophase of the investigated compounds. Light-induced changes in the texture and phase transition of the mesophase, attributed to the decrease of the order parameter due to *trans*–*cis* isomerization, have also been observed.

Received 24th May 2015
 Accepted 20th July 2015

DOI: 10.1039/c5ra09764a

www.rsc.org/advances

Introduction

Due to their ability to form polar order and phase chirality without chiral molecules, bent-core liquid crystals (BCLCs) offer exceptional properties (ferro-, antiferro-, piezo-, and flexoelectricity),^{1,2} which have high potential in both materials science and supramolecular chemistry. In recent years, significant attention has been devoted to azo-containing symmetric and asymmetric BCLCs,^{3–16} dimers combining rod-like and bent-core units,^{17,18} molecules with short core units containing four aromatic rings,^{19,20} and their side-chain polymers.^{21,22} Additionally, photoisomerizable chromophores that allow a change in the molecular conformation by a photoreaction may open up possibilities for polar responses modulated by light.

Asymmetric BCLCs with an azobenzene wing exhibit a variety of mesophases (N, B₁, B₂, B₇, SmA, SmA_dP_A *etc.*) over a wide temperature range.^{6,11–15} It has been shown that in a homologous series of asymmetric BCLCs, the lower homologues usually exhibit a B₁ and the higher ones a B₂ mesophase.¹¹ Even a small change in the molecular structure produces drastic changes in

their mesomorphic properties, *i.e.* the appearance, temperature range and nature of mesophase are governed by the types and the orientation of the linking group (ester, azomethine) between aromatic rings in the bent-core. Interestingly, the position of the azo group in the bent-core does not seem to affect the mesomorphic behaviour of BCLCs, whereas it has a profound effect on their photo-induced properties.¹² On the other hand, the clearing temperature and spontaneous polarization are more sensitive to light when the azo group is situated in the wings compared to cases where it is directly attached to the central phenyl ring. This can be attributed to a greater structural incompatibility in packing of the *cis* and *trans* isomers of the molecules in the layers of the former type of systems.

In BCLCs with resorcinol as the central ring and azobenzene with different alkoxy chain length as wings, the introduction of a large substituent in position 4 of the resorcinol moiety (CH₃, Br and I) together with an additional peripheral F-substituent favours the development of a new type of mesophase composed of chiral domains with opposite handedness (called dark conglomerate phases).^{7–9} The corresponding BCLCs with 4-chlororesorcinol form nematic and B₆ mesophases depending on the chain length,⁴ while the ones based on 4,6-dichlororesorcinol exhibit only a nematic mesophase.³ When resorcinol is replaced by the pyrimidine ring, the formation of a B₆ mesophase is observed.²³

Here we describe the chemical synthesis and physical characterizations of a new series of azo-containing asymmetric BCLCs (Fig. 1). The mesomorphic properties are varied by the type and length of the terminal chains, rigidity of wings, and by introducing a Cl-substituent into different positions on the bent-core. Almost all the compounds are found to be liquid

^aFaculty of Technology and Metallurgy, University of Belgrade, Karnegijeva 4, 11000 Belgrade, Serbia. E-mail: ntrisovic@tmf.bg.ac.rs

^bInstitute for Solid State Physics and Optics, Wigner Research Centre for Physics, Hungarian Academy of Sciences, Budapest, P.O.B. 49 H-152, Hungary

^cInstitute of Chemical Technology Prague, Technická 5, 166 28 Prague, Czech Republic

^dLiquid Crystal Institute, Kent State University, P.O. Box 5190, Kent, Ohio 44242-0001, USA

^eDepartment of Physics, Kent State University, P.O. Box 5190, Kent, Ohio 44242-0001, USA

† Electronic supplementary information (ESI) available: Synthetic procedures, spectral data for all new compounds, details of physical measurements and DSC thermographs. See DOI: 10.1039/c5ra09764a

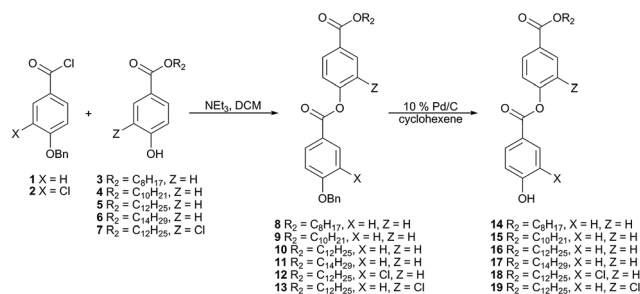
crystalline, exhibiting an enantiotropic modulated smectic (B₇ type) phase over relatively broad temperature ranges, and offering promise for potential applications.

Results and discussion

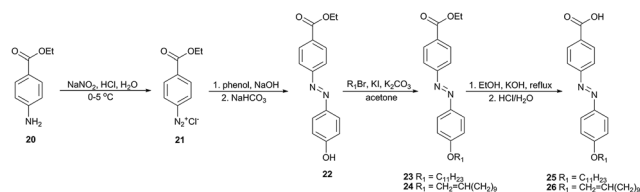
Synthesis

The studied asymmetric BCLCs were derived from 3-hydroxybenzoic acid, whereby their wings were obtained by the already known methodologies.^{5,24} The wing with the ester linking group between the phenyl rings (14–19) were prepared by an acylation of alkyl 3-substituted-4-hydroxybenzoates (3–7) with 3-substituted-4-benzyloxybenzoyl chloride (1, 2) and a subsequent deprotection of the intermediate esters 8–13 according to a literature procedure²⁴ (Scheme 1). In the synthesis of 4-alkoxyphenylazobenzoic acids (Scheme 2), ethyl 4-aminobenzoate (20) was firstly diazotized and the resulting diazonium salt (21) was coupled with phenol yielding ethyl 4-(4-hydroxyphenylazo)benzoate (22). The obtained compound 22 was alkylated with 1-bromoundecane or 11-bromo-1-undecene in the presence of potassium carbonate to give ester compounds (23, 24), which were further hydrolyzed under basic conditions to yield corresponding acids (25, 26). Similarly, (4-(11-undecenyl)oxyphenyl)azobenzoic acid (30) was prepared by diazotization of 4-aminobenzoic acid (27) and coupling of the resulting diazonium salt (28) with phenol yielding 4-hydroxyphenylazobenzoic acid (29) which was further acylated with 11-undecenyl chloride (Scheme 3).

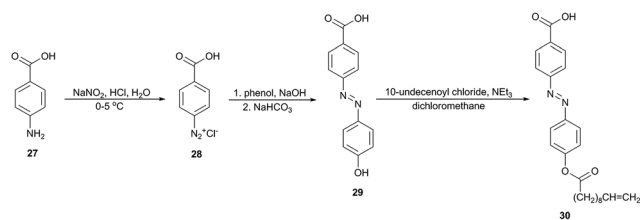
The synthesis of the target BCLCs was accomplished in three steps (Scheme 4). First, hydroxy esters 14–19 and dodecyl 4'-hydroxybiphenyl-4-carboxylate (32) were acylated by acid chloride of the protected central core 31. Subsequently, the benzylic protecting group was removed by transfer hydrogenation with cyclohexene and palladium on charcoal as a catalyst. In the last step, the hydroxy esters 40–46 were acylated by the acid chlorides of the second side wings 25, 26 and 30 affording the target materials **Ia–j**. BCLCs synthesized with the acids 26 and 30 possess a double bond in the terminal chain and they serve as model monomers for polymeric liquid crystals. The complete



Scheme 1 Synthesis of wings with the ester linking group (14–19).



Scheme 2 Synthesis of wings with the azo linking group (25, 26).



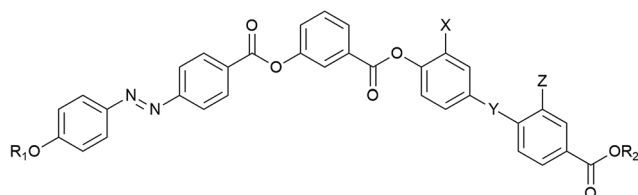
Scheme 3 Synthesis of the wing with the azo linking group (30).

synthetic procedures and analytical data are reported in the ESI.†

Calorimetric investigations

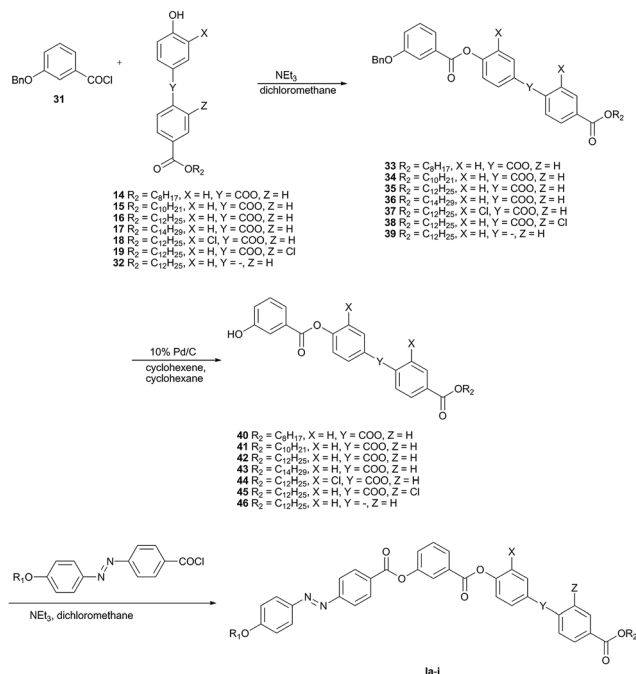
The thermal behaviour of the compounds has been studied by differential scanning calorimetry (DSC). Their transition temperatures (°C) measured at 5 °C min⁻¹ heating/cooling rates, the associated phase transition enthalpies (kJ mol⁻¹), and the phase sequences are presented in Table 1. All compounds are thermally stable as confirmed by the reproducibility of the thermographs in several heating and cooling cycles. Typical DSC thermographs taken on the second cooling run are shown in Fig. 2 for four selected compounds; the others are presented in Fig. S1.†

With exception of compound **Ih**, all compounds form the enantiotropic mesophase (M) over relatively broad temperature ranges. The transition temperatures of compounds **Ia–d** are nearly identical regardless of the length of the terminal chain R₂. A double bond in the terminal chain R₁ of compound **Ie** causes a slight decrease in the clearing temperature compared with **Ic**, whereas an ester group leads to an additional reduction of the mesophase temperature range (from 50 °C for **Ic** to 25 °C for **Ig**). When a Cl-substituent is introduced in the peripheral phenyl ring in the ester-containing wing (compound **Ii**), both



Compound	R ₁	R ₂	X	Y	Z
Ia	C ₁₁ H ₂₃	C ₈ H ₁₇	H	COO	H
Ib	C ₁₁ H ₂₃	C ₁₀ H ₂₁	H	COO	H
Ic	C ₁₁ H ₂₃	C ₁₂ H ₂₅	H	COO	H
Id	C ₁₁ H ₂₃	C ₁₄ H ₂₉	H	COO	H
Ie	CH ₂ =CH(CH ₂) ₉	C ₁₂ H ₂₅	H	COO	H
If	CH ₂ =CH(CH ₂) ₉	C ₁₄ H ₂₉	H	COO	H
Ig	CH ₂ =CH(CH ₂) ₈ C(=O)	C ₁₂ H ₂₅	H	COO	H
Ih	C ₁₁ H ₂₃	C ₁₂ H ₂₅	Cl	COO	H
Ii	C ₁₁ H ₂₃	C ₁₂ H ₂₅	H	COO	Cl
Ij	C ₁₁ H ₂₃	C ₁₂ H ₂₅	H	–	H

Fig. 1 Chemical structures of the investigated BCLCs.



Scheme 4 Synthesis of the target materials la–j

melting and clearing temperatures decrease for *ca.* 35 °C and the temperature range of the mesophase is narrowed. On the other side, introduction of a Cl-substituent in the phenyl ring located closer to the central ring destabilizes the mesophase and results in a crystalline compound **ih**.

X-ray results

The structures of mesophases were identified by small-angle X-ray diffraction (SAXS) measurements carried out on beamline 7.3.3 of the Advanced Light Source of Lawrence Berkeley National Lab (10 keV incident beam energy (1.24 Å wavelength), utilizing a Pilatus 2M detector) and at Structural Research Laboratory of University of Warsaw (BrukerNanoStar system with Vantec2000 detector, Cu K_α radiation (1.54 Å), equipped with heating stage).

The X-ray patterns recorded for all studied compounds show 2-D lattice structure corresponding either a columnar (B1)

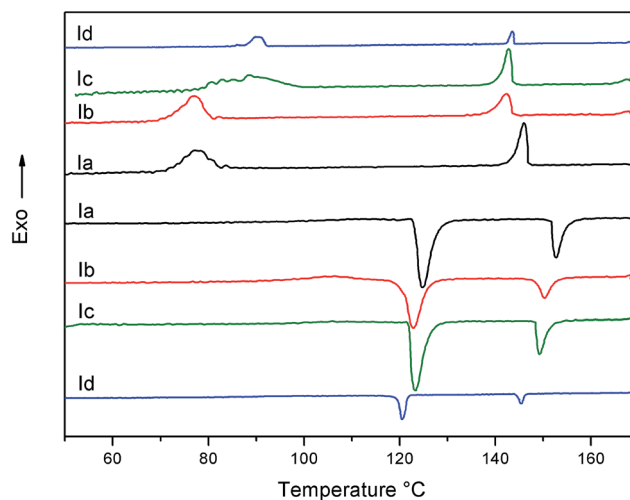


Fig. 2 DSC temperature plots for compounds la–ld detected at 5 °C min⁻¹ heating/cooling rates. The upper curves correspond to the second cooling and the corresponding lower curves to the second heating run.

phase, or a modulated smectic (B7) mesophase. The typical *q* dependence of the diffracted intensities in the peaks, and their corresponding Miller indices, are shown in Fig. 3.

The strongest signal indexed as (10) corresponds to electron density modulations parallel to the smectic layers with spacing $a = 2\pi/q_{(10)}$, that was found to be about 5.0 nm for all studied materials (see Tables 2 and S1†). The (01) peaks are an order of magnitude weaker than the (10) peaks and the corresponding $c = 2\pi/q_{(01)}$ periodicities are 2–4 times larger than of the (10) peaks (see Table 2). This type of pattern is similar to the so-called B₇ phase,^{25,26} in which the undulated layers are continuous through the polarization splay defects. However, when the layer undulation is so strong that the layers break into small ribbons, *i.e.*, the layer displacement steps at the defects,²⁷ it can be considered as a columnar (B1) structure.²⁸ A model structure of the molecular packing corresponding to this latter situation is shown in Fig. 3b. For recent reviews discussing modulated smectic and columnar phases, and the distinction between B1 and B7 structures, please see ref. 29–31. The angle β between the (10) and (01) peaks was found to be very close to 90° with the

Table 1 Transition temperatures (°C) and the enthalpies of transitions (kJ mol⁻¹) for the synthesized BCLCs

Compound	R ₁	R ₂	X	Y	Z	2nd Heating	2nd Cooling
la	C ₁₁ H ₂₃	C ₈ H ₁₇	H	COO	H	Cr 122.9 (-55.3) M 151.0 (-18.3) I	I 149.2 (19.1) M 81.4 (49.5) Cr
lb	C ₁₁ H ₂₃	C ₁₀ H ₂₁	H	COO	H	Cr 120.8 (-58.7) M 148.5 (-19.9) I	I 145.8 (20.6) M 81.0 (53.1) Cr
lc	C ₁₁ H ₂₃	C ₁₂ H ₂₅	H	COO	H	Cr 121.0 (-64.8) M 147.6 (-20.0) I	I 146.0 (21.8) M 94.0 (66.0) Cr
ld	C ₁₁ H ₂₃	C ₁₄ H ₂₉	H	COO	H	Cr 121.1 (-72.9) M 146.1 (-18.5) I	I 144.3 (21.3) M 86.4 (72.1) Cr
le	CH ₂ =CH(CH ₂) ₉	C ₁₂ H ₂₅	H	COO	H	Cr 113.2 (-57.1) M 141.7 (-18.9) I	I 139.6 (19.8) M 77.2 (52.1) Cr
lf	CH ₂ =CH(CH ₂) ₉	C ₁₄ H ₂₉	H	COO	H	Cr 113.0 (-59.7) M 141.1 (-17.8) I	I 139.2 (18.5) M 78.0 (68.9) Cr
lg	CH ₂ =CH(CH ₂) ₈ C(=O)	C ₁₂ H ₂₅	H	COO	H	Cr 127.0 (-46.0) M 138.9 (-13.8) I	I 136.9 (15.8) M 115.1 (50.1) Cr
lh	C ₁₁ H ₂₃	C ₁₂ H ₂₅	Cl	COO	H	Cr 125.5 (-64.9) I	I 120.8 (63.0) Cr
li	C ₁₁ H ₂₃	C ₁₂ H ₂₅	H	COO	Cl	Cr 97.9 (-42.2) M 105.0 (-14.4) I	I 103.8 (13.0) M 79.9 (41.4) Cr
lj	C ₁₁ H ₂₃	C ₁₂ H ₂₅	H	—	H	Cr 130.1 (-40.5) M 143.4 (-18.9) I	I 141.5 (20.4) M 101.4 (41.0) Cr

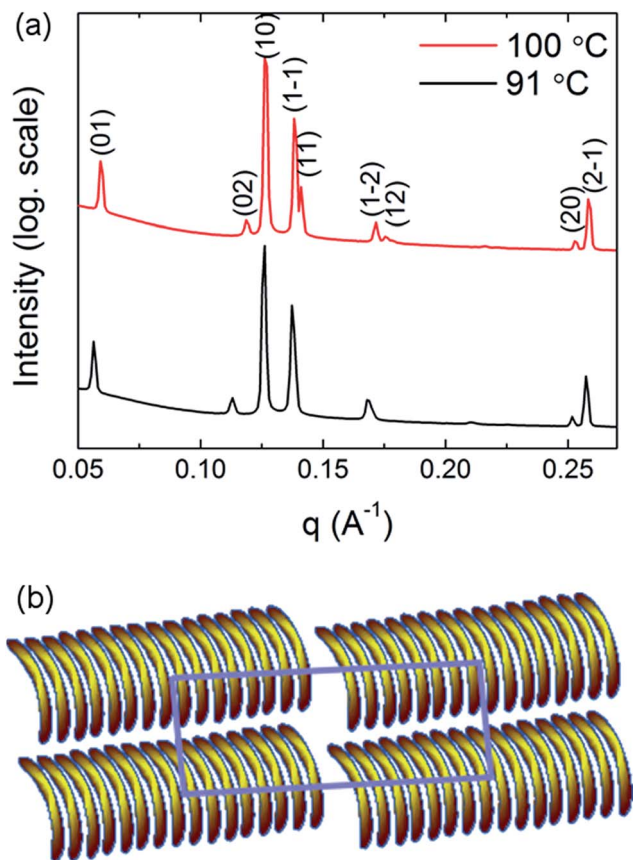


Fig. 3 (a) X-ray intensities vs. q for **1i** recorded at $T = 100\text{ °C}$ (red line) and at $T = 91\text{ °C}$ (black line) with corresponding Miller indices. (b) Suggested molecular packing. Note, the polar direction cannot be determined from X-ray measurements.

exception of **1c** where $\beta \sim 65^\circ$. The cell parameters at the high and low temperature ranges of the B_7 -type phase for all compounds are summarized in Table 2.

Table 2 The crystallographic unit cell parameters measured by X-ray in the B_7 -type phase at different temperatures

	T (°C)	a (Å)	c (Å)	β (deg)
1a	151	47.14	162.42	90
	103	48.43	122.98	90
1b	145	48.11	141.33	87.6
	110	48.27	196.22	88.1
1c	148	54.52	158.34	65.2
	112	52.63	208.75	71.7
1d	143	49.37	137.12	89.2
	91	50.15	233.21	88.0
1f	141	50.61	135.3	89.2
	107	51.67	180.39	89.6
1g	134	50.11	161.99	89.7
	117	50.15	218.98	89.6
1i	100	49.75	105.73	88.7
	91	49.91	112.02	89.4
1j	143	48.09	113.48	85.9
	113	49.14	145.79	88.4

Typical temperature dependencies of $q_{(10)}$ and $q_{(01)}$ are shown for compound **1d** in Fig. 4. One can see that while $q_{(10)}$ is only slightly increasing on cooling (for example $a(140\text{ °C}) = 4.95\text{ nm}$ and $a(90\text{ °C}) = 5.07\text{ nm}$), $q_{(01)}$ varies strongly ranging between 0.045 and 0.025 Å^{-1} in cooling, corresponding to variation of the periodicity the layer modulation in the range of $c \sim 12\text{--}22\text{ nm}$.

Polarizing optical microscopy studies

Typical POM textures are shown in Fig. 5. On cooling from the isotropic phase flower-like patterns grow and fill the space eventually. This texture is not typical for the classical B_7 phases with characteristic helical superstructures,²⁵ but rather similar to that of another asymmetric bent-core liquid crystal that possesses two ferroelectric mesophases.³² This dissimilarity might be related to the absence of large steric inclusions in the molecular cores, which are present in classical B_7 materials,³³ or indicates that the phase is rather a columnar phase.

We also tested the effect of light on the textures and phase transition. The result of the simple test when illuminated the sample by the light of a 100 W halogen lamp of the polarizing microscope ($I = 0.14\text{ W cm}^{-2}$) is shown in Fig. 5c and d zero and six minutes after the light was turned on. One clearly sees more isotropic areas after 6 minutes illumination, which shows the decrease of the order parameter due to the *trans-cis* isomerization of the molecules. More quantitative measurements to measure the optical effects are under way.

The fully developed mesophase in thin films of sample sandwiched between substrates treated for planar alignment show broken fan textures typical of smectic phases. The characteristic size of the smectic domains increases with slower cooling rates. A typical example for a planar texture formed under 0.1 °C min^{-1} cooling rate in $5\text{ }\mu\text{m}$ film is shown in Fig. 6. Although no polarization current peaks could be detected up to $50\text{ V }\mu\text{m}^{-1}$ fields, the birefringence of the films changed under

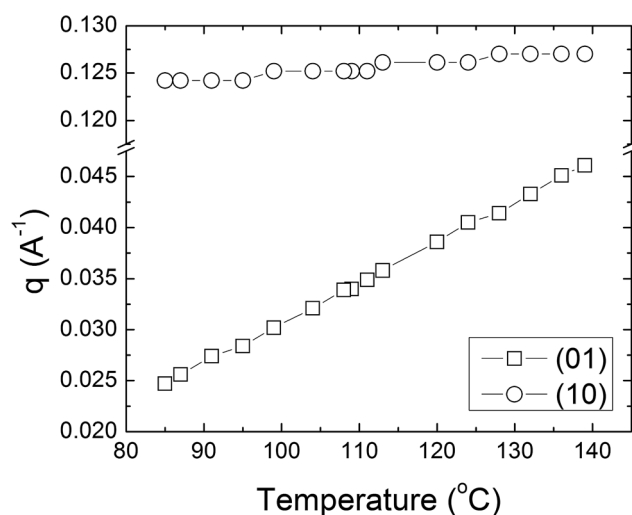


Fig. 4 Variation of q value of (01) and (10) signals vs. temperature for compound **1d**.

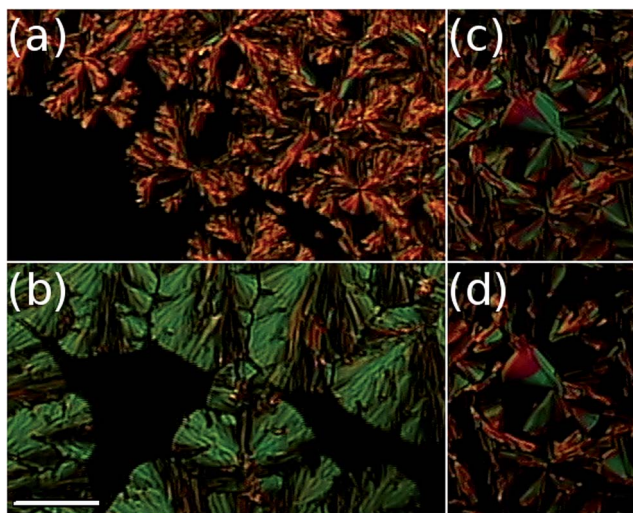


Fig. 5 Polarised optical microscopy textures in cooling during the phase transition from the isotropic to the B₇-type phase of **1a** at 106.6 °C (a) and **1a** at 150.5 °C (b). Texture of **1a** at $T = 106$ °C a few seconds (c), and 6 min (d) after the microscope light is turned on. Scale bar, 50 μm . Crossed polarizers are along the edges of the picture.

strong applied electric fields. This is illustrated for compound **1a** in Fig. 6b. After removal of the field, the birefringent texture was unchanged indicating that the electric field only caused

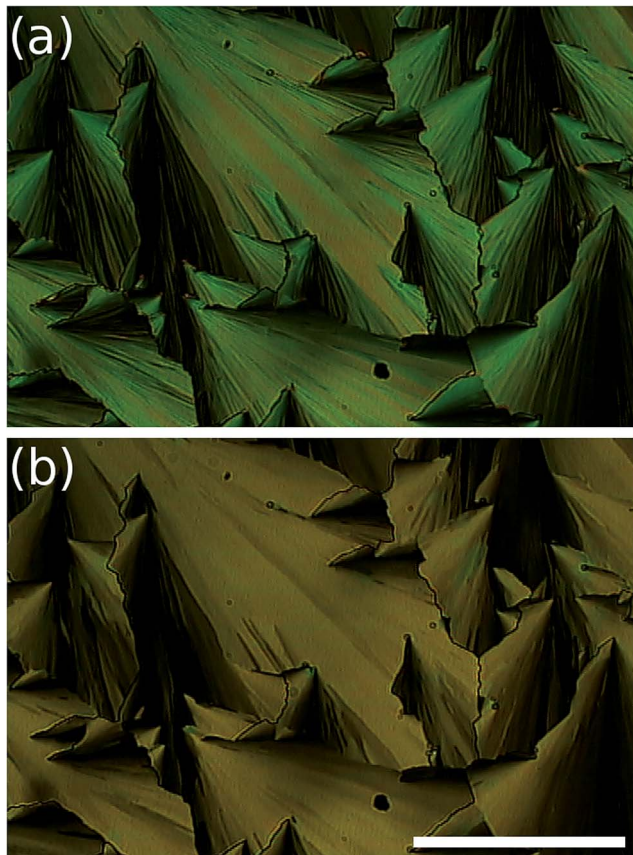


Fig. 6 Polarized optical microscopy texture of **1a** without electric field (a) and with electric field (ca. $55 \text{ V } \mu\text{m}^{-1}$). Scale bar, 150 μm . Crossed polarizers.

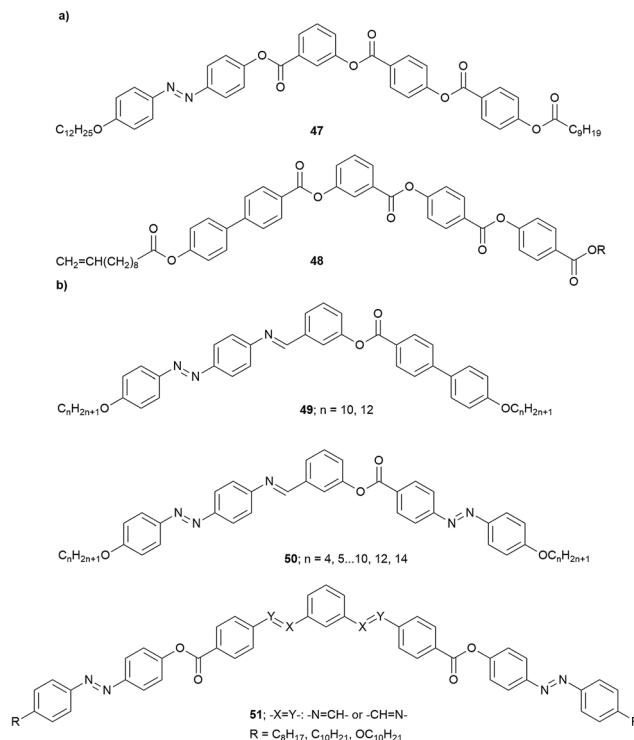


Fig. 7 (a) Structurally related BCLCs reported in the literature;^{11,24} (b) azo-containing BCLCs exhibiting a B₇ mesophase.^{6,13,16}

some realignment of the layers and was not related to ferroelectric switching.

Discussion

To make conclusions about structure–property relationships, we compare our materials with related compounds from the literature. Nagaveni *et al.* have reported that compound with the opposite orientation of the ester linking groups in the bent core (see **47** in Fig. 7a) does not have any liquid crystalline properties.¹¹ This is because the orientation of the ester linking groups has significant influence on the flexibility, polarity and bending angle of the molecules.³⁴ It has also been demonstrated that replacing the terminal alkanoyloxy chain in **47** with an alkyl or alkyloxy chain leads to BCLCs which exhibit a B₂ mesophase.¹⁴

Interestingly, the mesophase textures of our materials are rather similar to those of another asymmetric bent-core liquid crystal that possesses a single tilted synclinc ferroelectric ($\text{SmC}_s\text{P}_{\text{FE}}$) phase in a higher temperature range and an anti-ferroelectric ($\text{SmC}_s\text{P}_{\text{AF}}$) phase at lower temperatures^{24,32} (see material **48** of Fig. 7a). Furthermore even the clearing temperature of **48** is similar to our corresponding azo-compound **1g**.

There are only few examples of azo-containing BCLCs forming the B₇ mesophase. Srinivasan *et al.* have found that compound **49** (Fig. 7b) with a biphenyl unit exhibits an unusual B₇ mesophase, where different textures, like helical filaments, striped focal conics or fan-shaped, oval domains, myelinic and checkerboard textures have been observed.⁶ Compound **50** (Fig. 7b) with symmetrical wings exhibit an enantiotropic B₇

mesophase over about 15 °C the temperature range.¹³ A series of six-ring BCLCs (51 in Fig. 7b) is also shown to have a B₇ mesophase.¹⁶ Although characterized by a wide mesomorphic range (ca. 100 °C), these compounds possess very high clearing temperatures. The low and wide mesomorphic ranges of the compounds reported in this study might be useful for potential light sensitive applications.

Conclusions

In a search for new materials combining liquid crystalline and photochromic properties, we have presented the chemical synthesis and physical characterization of a new series of azo-containing asymmetric BCLCs. Almost all compounds form an enantiotropic layer modulated (B₇ type) phase. Interestingly, structural modifications, such as the type and length of the terminal chains, the rigidity of wings, and the presence of a Cl-substituent in the peripheral phenyl ring in the ester-containing wing, influence only the width of the mesomorphic temperature range, but not the type of the mesophase formed. The relatively low and wide photosensitive mesomorphic temperature range offers possible applications in such areas as high-density data storage systems, sensors, photonic switches and molecular logic gates.

Acknowledgements

This work was supported by the Serbian Ministry of Education, Science and Technological Development (Project no. 172013), Mera.Net [project MACOSYS (OTKA NN110672)]. Measurements at Berkeley and Kent were supported by NSF under grant DMR-1307674. The authors acknowledge important technical help and discussions from C. Zhu at the ALS, Lawrence Berkeley National Lab. M.S. acknowledges Prof. E. Gorecka (University of Warsaw) for the opportunity to perform an X-ray measurements.

Notes and references

- 1 T. Niori, T. Sekine, J. Watanabe, T. Furukawa, H. Takezoe, H. Sekine, T. Watanabe, J. Furukawa, T. Takezoe, T. S. T. Niori, J. Watanabe, T. Furukawa and H. Takezoe, *J. Mater. Chem.*, 1996, **6**, 1231.
- 2 J. Harden, B. Mbang, N. Éber, K. Fodor-Csorba, S. N. Sprunt, J. T. Gleeson and A. Jakli, *Phys. Rev. Lett.*, 2006, **97**, 157802.
- 3 M. Alaasar, M. Prehm and C. Tschierske, *Liq. Cryst.*, 2014, **41**, 126.
- 4 M. Alaasar, M. Prehm and C. Tschierske, *Liq. Cryst.*, 2013, **40**, 656.
- 5 C. L. Folcia, I. Alonso, J. Ortega, J. Etxebarria, I. Pintre and M. B. Ros, *Chem. Mater.*, 2006, **18**, 4617.
- 6 M. V. Srinivasan, P. Kannan and A. Roy, *New J. Chem.*, 2013, **37**, 1584.
- 7 M. Alaasar, M. Prehm, M. Brautzsch and C. Tschierske, *J. Mater. Chem. C*, 2014, **2**, 5487.
- 8 M. Alaasar, M. Prehm, M. Brautzsch and C. Tschierske, *Soft Matter*, 2014, **10**, 7285.
- 9 M. Alaasar, M. Prehm and C. Tschierske, *Chem. Commun.*, 2013, **49**, 11062.
- 10 M. Alaasar, M. Prehm, K. May, A. Eremin and C. Tschierske, *Adv. Funct. Mater.*, 2014, **24**, 1703.
- 11 N. G. Nagaveni, A. Roy and V. Prasad, *J. Mater. Chem.*, 2012, **22**, 8948.
- 12 N. G. Nagaveni, P. Raghuvanshi, A. Roy and V. Prasad, *Liq. Cryst.*, 2013, **40**, 1238.
- 13 N. G. Nagaveni, V. Prasad and A. Roy, *Liq. Cryst.*, 2013, **40**, 1405.
- 14 V. Prasad, S.-W. Kang, X. Qi and S. Kumar, *J. Mater. Chem.*, 2004, **14**, 1495.
- 15 V. Prasad and A. I. Jakli, *Liq. Cryst.*, 2004, **31**, 473.
- 16 V. Prasad, *Mol. Cryst. Liq. Cryst.*, 2001, **363**, 167.
- 17 N. G. Nagaveni, V. Prasad and A. Roy, *Liq. Cryst.*, 2013, **40**, 1001.
- 18 N. Sebastián, N. Gimeno, J. Vergara, D. O. López, J. L. Serrano, C. L. Folcia, M. R. de la Fuente and M. B. Ros, *J. Mater. Chem. C*, 2014, **2**, 4027.
- 19 N. Begum, S. Turlapati, S. Debnath, G. Mohiuddin, D. D. Sarkar and V. S. R. Nandiraju, *Liq. Cryst.*, 2013, **40**, 1105.
- 20 S. Debnath, G. Mohiuddin, S. Turlapati, N. Begum, D. D. Sarkar and V. S. N. Rao, *Dyes Pigm.*, 2013, **99**, 447.
- 21 M. V. Srinivasan, P. Kannan and A. Roy, *J. Polym. Sci., Part A: Polym. Chem.*, 2013, **51**, 936.
- 22 N. Gimeno, I. Pintre, M. Martínez-Abadía, J. L. Serrano and M. B. Ros, *RSC Adv.*, 2014, **4**, 19694.
- 23 M. L. Rahman, G. Hegde, M. M. Yusoff, M. N. F. A. Malek, H. T. Srinivasa and S. Kumar, *New J. Chem.*, 2013, **37**, 2460.
- 24 M. Kohout, M. Chambers, A. Vajda, G. Galli, A. Domjan, J. Svoboda, A. Bubnov, A. Jakli and K. Fodor-Csorba, *Liq. Cryst.*, 2010, **37**, 537.
- 25 G. Pelzl, S. Diele, A. Jakli, C. H. Lischka, I. Wirth and W. Weissflog, *Liq. Cryst.*, 1999, **26**, 135.
- 26 G. Pelzl, S. Diele, A. Jakli and W. Weissflog, *Liq. Cryst.*, 2006, **33**, 1513.
- 27 D. A. Coleman, C. D. Jones, M. Nakata, N. A. Clark, D. M. Walba, W. Weissflog, K. Fodor-Csorba, J. Watanabe, V. Novotna and V. Hamplova, *Phys. Rev. E: Stat., Nonlinear, Soft Matter Phys.*, 2008, **77**, 021703.
- 28 C. L. Folcia, J. Etxebarria, J. Ortega and M. B. Ros, *Phys. Rev. E: Stat., Nonlinear, Soft Matter Phys.*, 2005, **72**, 41709.
- 29 A. Eremin and A. Jakli, *Soft Matter*, 2013, **9**, 615.
- 30 N. Gimeno and M. B. Ros, in *Handbook of Liquid Crystals*, ed. J. W. Goodby, P. J. Collings, T. Kato, C. Tschierske, H. F. Gleeson and P. Raynes, Wiley-VCH Verlag, Weinheim, Germany, 2014, pp. 605–679.
- 31 E. Gorecka, D. Pocięcha and N. Vaupotic, in *Handbook of Liquid Crystals*, ed. J. W. Goodby, P. J. Collings, T. Kato, C. Tschierske, H. F. Gleeson and P. Raynes, Wiley-VCH Verlag, Weinheim, Germany, 2014, pp. 743–768.
- 32 C. Zhang, N. Diorio, S. Radhika, B. K. K. Sadashiva, S. N. Sprunt and A. Jakli, *Liq. Cryst.*, 2012, **39**, 1149.
- 33 C. A. Bailey and A. Jakli, *Phys. Rev. Lett.*, 2007, **99**, 207801.
- 34 S. A. R. Krishnan, W. Weissflog, G. Pelzl, S. Diele, H. Kresse, Z. Vakhovskaya and R. Friedemann, *Phys. Chem. Chem. Phys.*, 2006, **8**, 1170.